

RESEARCH PAPER

Osteoprotegerin disrupts peripheral adhesive structures of osteoclasts by modulating Pyk2 and Src activities

Hongyan Zhao^{a,b,†}, Xuezhong Liu^{a,b,†}, Hui Zou^{a,b}, Nannan Dai^{a,b}, Lulian Yao^{a,b}, Xiao Zhang^{a,b}, Qian Gao^{a,b}, Wei Liu^{a,b}, Jianhong Gu^{a,b}, Yan Yuan^{a,b}, Jianchun Bian^{a,b}, and Zongping Liu^{a,b}

^aCollege of Veterinary Medicine, Yangzhou University, Yangzhou, Jiangsu, P.R. China; ^bJiangsu Co-innovation Center for Prevention and Control of Important, Animal Infectious Diseases and Zoonoses, Yangzhou, Jiangsu, P.R. China

ABSTRACT

Osteoprotegerin has previously been shown to modulate bone mass by blocking osteoclast maturation and function. The detailed mechanisms of osteoprotegerin-induced disassembly of podosomes, disruption of adhesive structures and modulation of adhesion-related proteins in osteoclasts, however, are not well characterized. In this study, tartrate-resistant acidic phosphatase staining demonstrated that osteoprotegerin inhibited differentiation of osteoclasts. The use of scanning electron microscopy, real-time cell monitoring and confocal microscopy indicated that osteoclasts responded in a time and dose-dependent manner to osteoprotegerin treatments with retraction of peripheral adhesive structures and detachment from the extracellular substrate. Combined imaging and Western blot studies showed that osteoprotegerin induced dephosphorylation of Tyr 402 in Pyk2 and decreased its labeling in peripheral adhesion regions. Osteoprotegerin induced increased intracellular labeling of Tyr 402 in Pyk2, Tyr 416 in Src, increased dephosphorylation of Tyr 527 in Src, and increased Pyk2/Src association in the central region of osteoclasts. This evidence suggests that Src may function as an adaptor protein that competes for Pyk2 and relocates it from the peripheral adhesive zone to the central region of osteoclasts in response to osteoprotegerin treatment. Osteoprotegerin may induce podosome reassembly and peripheral adhesive structure detachment by modulating phosphorylation of Pyk2 and Src and their intracellular distribution in osteoclasts.

ARTICLE HISTORY

Received 1 June 2015
Revised 29 October 2015
Accepted 4 December 2015

KEYWORDS

osteoclast; osteoprotegerin; podosome; Pyk2; src



Introduction

Mature bones that comprise the skeletons of mammals are composed of a complex mixture of organic and inorganic materials. Proper maintenance of bone matrix is regulated by the opposing activities of 2 major types of cells: osteoclasts (OCs), which remove bone, and osteoblasts, which lay down the new organic matrix on which mineralization occurs. Bone mass is stable when the amount of bone removed by OCs is evenly balanced by osteoblastic bone formation.^{1,2} Excessive OC formation and bone resorption are closely related with diseases such as osteoporosis, periodontitis and tooth loss.^{3,4}

OCs are multinucleated cells of the monocyte-macrophage lineage, and are derived from haematopoietic stem cells through a series of differentiation steps.⁵ Two essential cytokines, macrophage colony-stimulating factor (M-CSF) and receptor activator of NF- κ B ligand (RANKL),

play a central role in bone destructive disorders. M-CSF supports proliferation and survival of precursor cells during OC differentiation while RANKL, a TNF family cytokine that binds to the receptor RANK, promotes OC formation from OC precursors.^{6,7} Osteoprotegerin (OPG), a member of the tumor necrosis factor (TNF)/TNF receptor superfamily, is a decoy receptor for the pro-osteoclastic cytokine RANKL with an equivalently high affinity as RANKL for its receptor RANK.^{8,9} OPG/RANKL binding prevents the interaction of RANKL with RANK, which is expressed on the cell surface of OC precursors, and thus inhibits OC differentiation.² OPG knockout mice display osteoporosis owing to enhanced bone resorption at local sites. The decreased activity by OCs induced by exogenous OPG may improve bone mass.¹⁰

Adherence of OCs to bone matrix activates integrin molecules and results in increased phosphorylation of podosomal-associated proteins, such as Pyk2, c-Src, paxillin,

CONTACT Zongping Liu  liuzongping@yzu.edu.cn  President's Office, College of Veterinary Medicine, Yangzhou University, 12 Wenhui East Road, Yangzhou, Jiangsu 225009, P. R. China.

Color versions of one or more figures in this article can be found online at www.tandfonline.com/kcam.

[†]These authors contributed equally to this work

© 2016 Taylor & Francis

p130cas, and Cbl. Phosphorylation-related effects affect the activities of WASP, cortactin, and other actin-interacting molecules, and ultimately lead to OC adhesion/migration, organization of the sealing zone, and vesicular trafficking.¹¹ The proteins and cellular mechanisms that regulate podosome belt formation are not well understood. In OCs, Pyk2 is localized to the podosome belt and deletion of Pyk2 leads to an impairment of OC function, which in part contributes to the osteopetrotic phenotype observed in Pyk2-deficient mice.^{12,13} Tyrosine 402 in Pyk2 has been suggested as the primary autophosphorylation site providing a docking site for the SH2 domain of c-Src.¹⁴⁻¹⁶ Src, a non-receptor protein-tyrosine kinase, plays an important role in cell adhesion, cell morphology and motility, and bone resorption. Focal adhesion kinase (FAK) and the Crk and Src associated substrate (Cas) are focal adhesion proteins important for integrin signaling and are substrates of Src.¹⁷ From its N- to C-terminus, Src contains a 14-carbon myristoyl group attached to an SH4 domain, a unique domain, an SH3 domain, an SH2 domain, an SH2-kinase linker, a protein-tyrosine kinase domain (the SH1 domain), and a C-terminal regulatory segment.¹⁸ One of the 2 most important regulatory phosphorylation sites in Src is Tyr 527, 6 residues from the C-terminus. Under basal conditions *in vivo*, 90–95% of Src is phosphorylated at Tyr 527¹⁹ and phosphotyrosine 527 binds intramolecularly with the Src SH2 domain. This intramolecular association stabilizes a restrained form of the enzyme.¹⁸ Src undergoes an intermolecular autophosphorylation at Tyr 416; this residue is present in the activation loop, and its phosphorylation promotes kinase activity.¹⁸

In the present study, tartrate-resistant acidic phosphatase (TRAP) staining was used to determine the inhibitory effects of OPG on differentiation of OCs. We used scanning electron microscopy (SEM) and a real-time cell analyzer (RTCA) to assess the effects of OPG on adhesion structures in living OCs. We found that the OCs responded to OPG treatment in a time and dose-dependent manner with retraction of adhesive structures in the peripheral region and detachment from the extracellular substrate. Combined imaging and Western blot studies, which showed the occurrence of the retraction process correlated well with a decrease in the levels of tyrosine phosphorylation at Tyr 402 in Pyk2 and Tyr 527 in Src and an increase in tyrosine phosphorylation at Tyr 416 in Src, suggest that Pyk2 and Src are involved in the retraction effects induced by OPG in OCs.

Materials and methods

Antibodies and chemicals

Tartrate-resistant acid phosphatase (TRAP) Kit 387-A, rhodamine-phalloidin, 4'6-diamidino-2-phenylindole

(DAPI) and mouse anti-Vinculin antibody were purchased from Sigma Chemical Co. (St. Louis, MO, USA). Dulbecco's modified Eagle's medium (DMEM), minimum essential medium α (α -MEM) and fetal bovine serum (FBS) were obtained from Gibco Laboratories (Grand Island, NY, USA). M-CSF, RANKL and OPG were obtained from Peprotech Inc. (Rocky Hill, NJ, USA). Collagen I was obtained from BD Biosciences (Bedford, MA, USA). Rabbit anti-Pyk2, anti-Src, anti-Src phosphotyrosine residue 416, anti-Src phosphotyrosine residue 527, anti- β -actin antibodies and mouse anti-phosphotyrosine, anti-Pyk2 phosphotyrosine residue 402 antibodies were obtained from Cell Signaling Technology Inc. (Danvers, MA, USA). Goat anti-Pyk2, horseradish peroxidase (HRP)-conjugated goat anti-rabbit IgG, fluorescein isothiocyanate (FITC)-conjugated goat anti-rabbit IgG, FITC-conjugated goat anti-mouse IgG, FITC-conjugated donkey anti-goat IgG and Cy3-conjugated goat anti-rabbit IgG were purchased from Santa Cruz Biotechnology Inc. (Dallas, TX, USA).

Cell culture and treatment

Mouse monocyte RAW264.7 cells were obtained from American Type Culture Collection (ATCC, Manassas, VA, USA) and cultured in DMEM supplemented with 10% FBS, 100 U/mL penicillin, 100 μ g/mL streptomycin and 2 mmol/L L-glutamine. To generate OCs, RAW264.7 cells were suspended in α -MEM containing 10% FBS, and differentiated with the addition of 30 ng/mL RANKL and 25 ng/mL M-CSF as previously described.²⁰ After 48 h of incubation, the medium was changed to serum-free α -MEM with the addition of RANKL and M-CSF. Following an additional 24 h incubation, 0, 20, 40 or 80 ng/mL OPG was added and the cells were incubated for an additional 24 h.

Impedance measurements with the xCelligence system

Background impedance was determined in 100 μ L medium followed by measurement of 100 μ L of the RAW264.7 cell suspension (2000 cells/well). Cells were incubated for 30 min at room temperature (RT) and E-plates were placed into the Real-Time Cell Analyzer (RTCA). Impedance was monitored every 15 min using the xCELLigence system. After 3 days, cells were incubated with different concentrations of OPG (0, 20, 40 or 80 ng/mL). Impedance was represented by the cell index (CI) values $((Z_t - Z_0) [\text{Ohm}]/15[\text{Ohm}])$; Z_0 : background resistance, Z_t : individual time point resistance) and the normalized cell index was calculated as the cell index CI_{t_i}

at a given time point divided by the cell index $CI_{\text{nml_time}}$ at the normalization time point (nml_time).

TRAP staining

RAW 264.7 cells were seeded at a density of 2×10^4 cells/well in 24-well plates coated with 0.6 mg/mL collagen I. After a 3-day incubation, cells were incubated with different concentrations of OPG (0, 20, 40 and 80 ng/mL) for 24 h. Thereafter, cells were processed according to the instructions of the TRAP staining kit. The mature OC cytoplasm was dyed to a typical rose red color and contained 3 or more nuclei which were colored dark blue or blue-violet. The number of OCs that stained positive for TRAP was determined as the mean value of 10 visual fields in different areas of at least 3 wells under an inverted phase contrast microscope (DMI3000B; Leica).

Scanning electron microscopy (SEM)

RAW 264.7 cells were seeded at a density of 2×10^4 cells/well in 24-well plates containing coverslips with or without 0.6 mg/mL collagen I. Following a 3-day incubation, cells were incubated with different concentrations of OPG (0, 20, 40 or 80 ng/mL) for 24 h. Cells that were adhered to the glass coverslips were fixed in 2.5% glutaraldehyde solution overnight at 4°C, dehydrated using increasing concentrations of ethanol from 50 to 100% , and dried. To observe morphologies, the specimens were coated with gold using a SCD 500 sputter-coater and examined using a Hitachi S-4800 Field-Emission Environmental Scanning Electron Microscope at various magnifications.

Immunostaining and confocal microscopy

OCs on coverslips were fixed with 4% paraformaldehyde in PBS for 30 min at RT and permeabilized for 20 min with 0.5% Triton X-100 in PBS. The coverslips were then blocked in 5% normal goat serum for 20 min, and incubated with the appropriate primary antibody diluted in 2% BSA-PBS overnight at 4°C. Thereafter, cells were washed in PBS, incubated for 1 h with the appropriate Cy3/FITC-conjugated secondary antibody, and washed. F-actin was stained with rhodamine phalloidin at a 1:40 dilution (in PBS) and nuclei visualized using 1 $\mu\text{g/mL}$ DAPI. Cells were examined using a scanning laser confocal imaging system (LSM 710; ZEISS). Images were recorded, composite images were compiled, and image enhancements performed using Adobe Photoshop CS2.

Western blotting analysis

RAW 264.7 cells were seeded at a density of 6×10^4 cells/well in 6-well plates coated with 0.6 mg/mL collagen I. Following a 3-day incubation, cells were incubated with different concentrations of OPG (0, 20, 40 and 80 ng/mL) for 24 h. After treatment, cells were washed twice with cold PBS and lysed in RIPA buffer on ice for 30 min. Lysates were sonicated for 10 s and centrifuged at 12,000 g for 10 min at 4°C. Protein concentration was determined using the BCA protein assay kit. Lysate aliquots were diluted with 6 \times sodium dodecyl sulfate (SDS) sample buffer and boiled for 10 min. Equivalent amounts of protein were separated on 8–10% SDS-polyacrylamide gels and transferred to nitrocellulose membranes. Membranes were incubated with TBS containing 0.05% Tween 20 and 5% nonfat dry milk to block non-specific binding. After incubation with primary and peroxidase-coupled secondary antibodies, bound antibodies were detected by chemiluminescence (ECL, Amersham).

Statistical analysis

All experimental values were expressed as the mean \pm standard deviation (SD) of 3 independent experiments. Statistical differences between groups were evaluated by Student's t-test using SPSS v.17.0 software. $P < 0.05$ was considered statistically significant.

Results

OPG inhibits differentiation of OCs

M-CSF and RANKL induced a high degree of TRAP-positive, multinucleated OC differentiation in RAW264.7 cells *in vitro* (Fig. 1A), indicating that these cells were mature OCs. OPG was added to RAW264.7 cells stimulated with M-CSF and RANKL for 24 h. OPG decreased the formation of TRAP-positive mononucleated OCs (Fig. 1A) in a dose-dependent manner by $30.00 \pm 6.47\%$, $51.00 \pm 3.53\%$ and $73.67 \pm 6.37\%$ at OPG concentrations of 20, 40 and 80 ng/mL, respectively (Fig. 1B).

OPG induces retraction of adhesive structures at the peripheral region in OCs

SEM allowed us to analyze the morphological changes of adhesion structures in OCs. RAW264.7 cells, cultured in DMEM as described in the methods, showed the typical appearance characteristics of monocytes, which are quite different from OCs in terms of size and adhesive structures (Fig. 2A, panel a). Adhesion structures (podosomes) distributed as a circular zone near the periphery of the cell (Fig. 4A, upper panel labeled actin). Outside

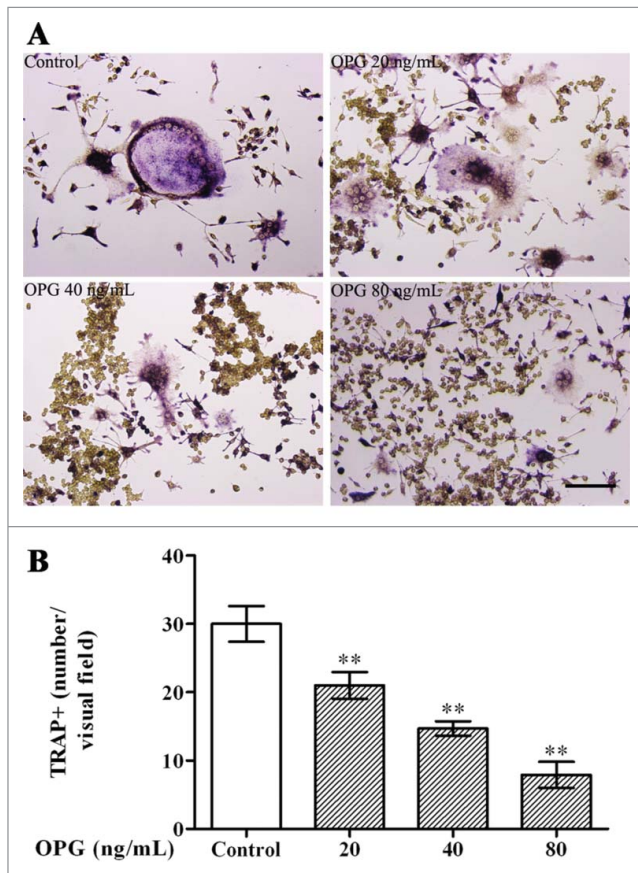


Figure 1. Inhibitory effects of OPG on osteoclast differentiation. RAW264.7 cells were suspended in α -MEM containing 10% FBS, 30 ng/mL RANKL and 25 ng/mL M-CSF. After 48 h of incubation, the medium was changed to serum-free α -MEM containing the 2 cytokines the cells were cultured for an additional 24 h. Next, OPG (0, 20, 40 and 80 ng/mL) was added and incubated for 24 h. (A) Cells were fixed and stained for TRAP (Magnification $\times 200$, Scale bar = 50 μ m) (B) TRAP-positive multinucleated cells (TRAP+) were observed by inverted phase contrast microscopy and counted (Magnification $\times 100$). The results are expressed as the mean \pm SD. ** $p < 0.01$ and * $p < 0.05$ versus control.

this peripheral circular zone, protrusions of lamellipodia (white arrows), and many thin filopodia (white arrowheads) could be observed (Fig. 2A, panel c). OCs cultured on collagen I-coated coverslips show more lamellipodia and filopodia compared with OCs cultured on coverslips (Fig. 2A, panels b, c). OPG caused a dose-dependent series of morphological changes in OCs (Fig. 2A, panels d-f). 20 ng/mL OPG only triggered the retraction of lamellipodia. While, cells treated with 40 and 80 ng/mL OPG showed more severe retraction of lamellipodia and longer filopodia-like structures, thus cells rounded up and detached from the substrate.

We next determined whether the kinetics of morphological changes could be monitored in real time by using impedance-based cell analysis. To assess the effects of M-CSF and RANKL in the presence or absence of OPG on

the functional status of RAW264.7, CI was recorded. CI is a quantitative measure of cell status in a well, including the cell number, cell viability, degree of adhesion, and morphology. The "Normalized cell index (NCI)" at a certain time point is acquired by dividing the CI value by the value at a reference time point. M-CSF and RANKL induced OC differentiation, but inhibited proliferation of RAW264.7 cells (Fig. 2B); therefore, the NCI of the control is lower than the NCI of RAW264.7 cells. Treatment with OPG at the concentrations tested decreased the CI of OCs in a dose-dependent manner beginning approximately 3 hours after treatment (Fig. 2B).

OPG-induced signaling modulates tyrosine phosphorylation in Pyk2 and Src and modulates their association in OCs

We examined changes in Pyk2 tyrosine phosphorylation after OPG treatment of OCs cultured in 6-well plates with collagen-I coating. As shown in Figure 3A and B, OPG causes a reduction in phosphorylation. Phosphorylation of Tyr 402 in Pyk2 is important for OC spreading and adhesion-induced association of Pyk2 with c-Src.²¹ Therefore, we examined the effect of OPG on this event. Treatment with OPG decreased phosphorylation of Tyr 402 in Pyk2 in a dose-dependent manner in OCs (Figs. 3A and B). Thereafter, as shown in Figure 3C–D, tyrosine phosphorylation in Src increased after treatment with 20 ng/mL OPG, then decreased at 80 ng/mL OPG. OPG induced significant increases in Src Tyr 416 phosphorylation and, unexpectedly, a decrease in Src Tyr 527 phosphorylation at a concentration of 80 ng/mL OPG (Figs. 3C and D). These results suggest that the OPG-induced retraction of OCs may be accompanied by decreased tyrosine phosphorylation in Pyk2 and increased tyrosine phosphorylation in Src.

OPG induced redistribution of podosomes, Pyk2, and Src from the peripheral adhesion zone toward the central region of OCs

To gain further insights into the mechanism underlying the dysfunction of OCs induced by OPG, especially regarding the possible involvement of Pyk2 and Src in OPG-induced OC retraction, confocal microscope analysis of immunofluorescent labeling of actin, vinculin, Pyk2, and Src in OCs was performed. Most of the actin-containing podosomes and vinculin, Pyk2, and Src were localized to the peripheral adhesive region in the control group (Figs. 4B, E, F, upper panel). OPG treatment induced disruption of the peripheral distribution of ring-like, actin-containing podosome structures, vinculin, Pyk2 and Src. Labeling of vinculin, Pyk2 and Src was

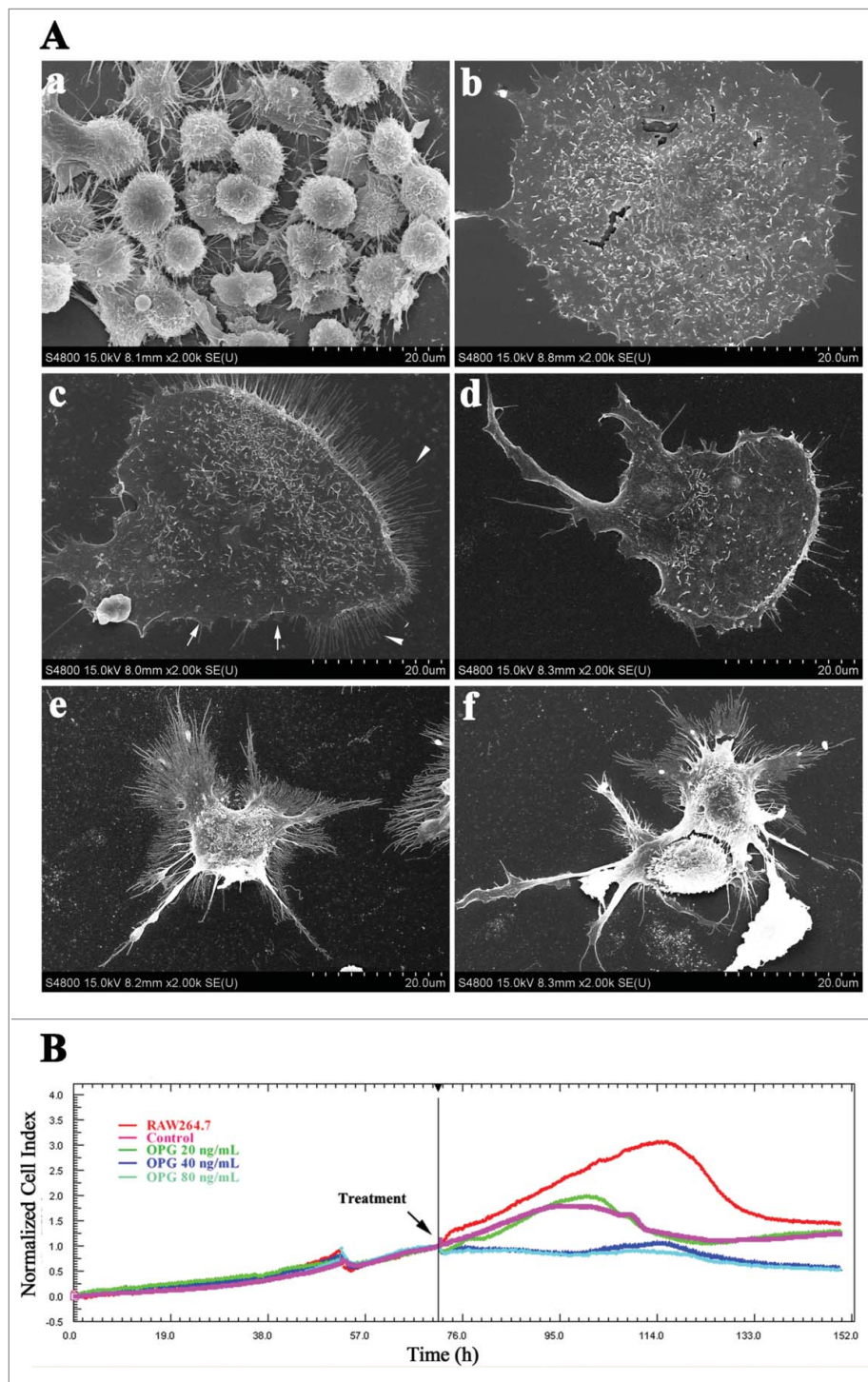


Figure 2. Retraction of adhesive structures in OCs induced by OPG. (A) OPG-induced adhesive region detachment in OC examined by SEM. OCs were cultured on glass coverslips with (c-f) or without (a, b) collagen-I treatment. Various concentrations of OPG (0 (b, c), 20 (d), 40 (e) and 80 (f) ng/mL) were added for 24 h. White arrows indicate lamellipodia; white arrowheads indicate filopodia. (B) Dynamic monitoring of OCs treated with OPG using impedance technology. Cell index (CI) values were normalized to the time point of administration. Black arrow: OPG addition. Representative data are averaged from 3 wells. All experiments were repeated at least 3 times.

diffuse inside OCs and more vinculin, Pyk2 and Src was localized away from podosomes than in control cells (Figs. 4B, E-F, lower panel). OPG-induced signaling modulated the state of Pyk2 and Src tyrosine phosphorylation; therefore, OPG-induced changes in the

intracellular distribution of phosphorylated Pyk2 and Src in OCs were examined. Actin-containing podosomes, phosphorylated Tyr 402 Pyk2, and Tyr 527 Src were highly co-localized in the peripheral adhesion zone of OCs in the control group (Figs. 4A, D upper panel).

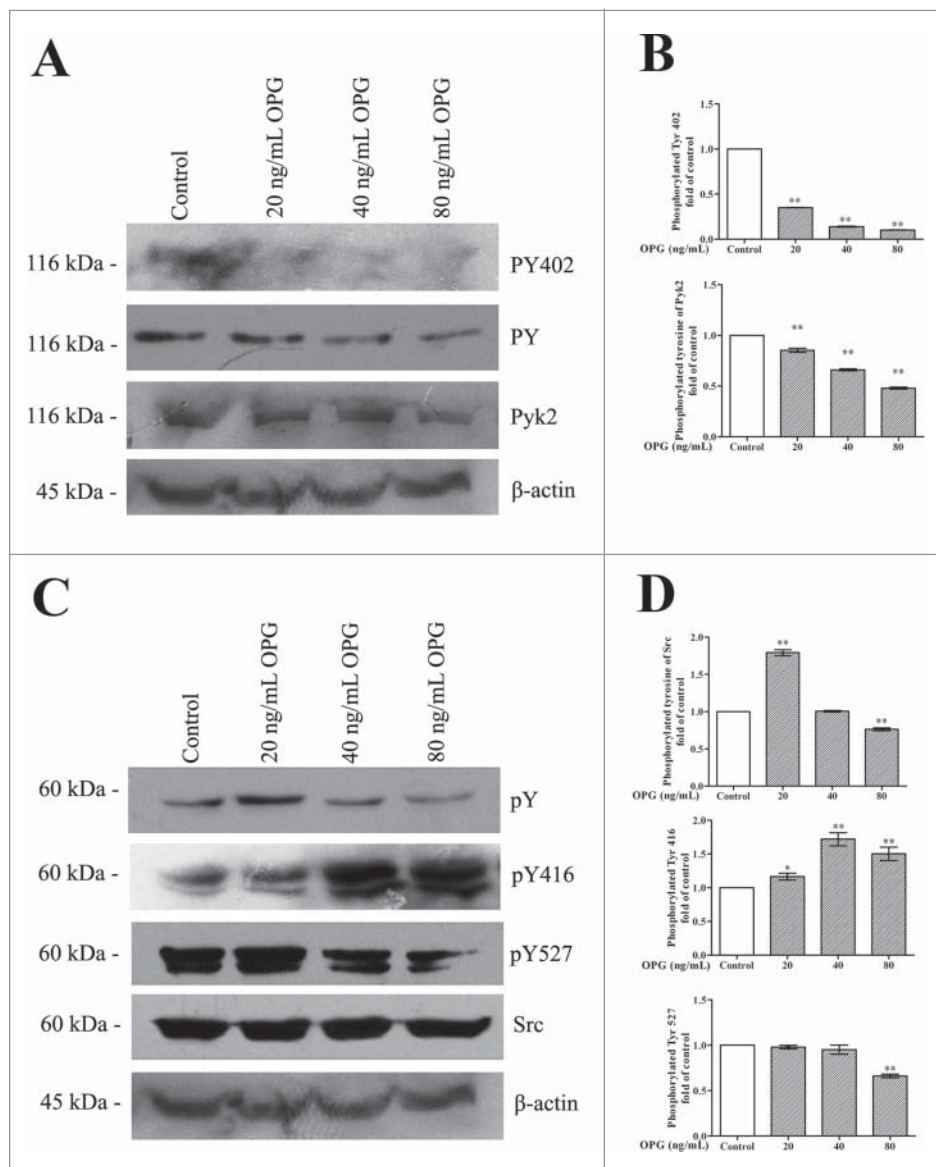


Figure 3. OPG-induced dose-dependent decrease in tyrosine phosphorylation in Pyk2 and activation of Src. OCs were cultured in 6-well plates with collagen I coating and treated with the indicated amount of OPG for 24 h. (A) OCs were lysed and immunoblotted with anti-phosphotyrosine antibody, anti-Pyk2 antibody, anti-Pyk2 phosphotyrosine 402 antibody and β -actin antibody. (C) The proteins were subjected to Western blotting with anti-phosphotyrosine antibody and an anti-Pyk2 antibody. The membrane was then stripped and reprobed with an anti-Src antibody, anti-Src pTyr 416 antibody, anti-Src pTyr 527 antibody, anti-Src antibody and anti- β -actin antibody as a loading control. (B, D) The amount of protein was quantified by densitometry, and was corrected for sample loading based on the amount of protein and expressed as fold increase or decrease relative to the control lane. Each blot is representative of at least 3 replicate experiments.

OPG disrupted phosphorylated Tyr 402 Pyk2 and Tyr 527 Src in the peripheral region of OCs. Less immunostaining for phosphorylated Tyr 402 Pyk2 and Tyr 527 Src was noted in OPG-treated cells. OPG treatment caused decreased Tyr 402 Pyk2 and Tyr 527 Src labeling in peripheral and central regions, and disrupted their co-localization with podosomes in both regions (Figs. 4A-D, lower panel). As shown in the upper panel of Figure 4C, co-localization of phosphorylated Tyr 416 Src and podosomes at the peripheral and central regions of OCs was

noted in the control group. More immunostaining for phosphorylated Tyr 416 Src was noted in OPG-treated cells. OPG treatment caused an increase in Tyr 416 Src labeling at peripheral and central regions, and disrupted their co-localization with podosomes in both regions (Fig. 4C, lower panel).

As OPG induced redistribution of Pyk2 and Src, the heterogeneity of localization between them was explored. Either phosphorylated Tyr 402 Pyk2 or Pyk2 was highly colocalized with Src at peripheral adhesion zone of OCs in

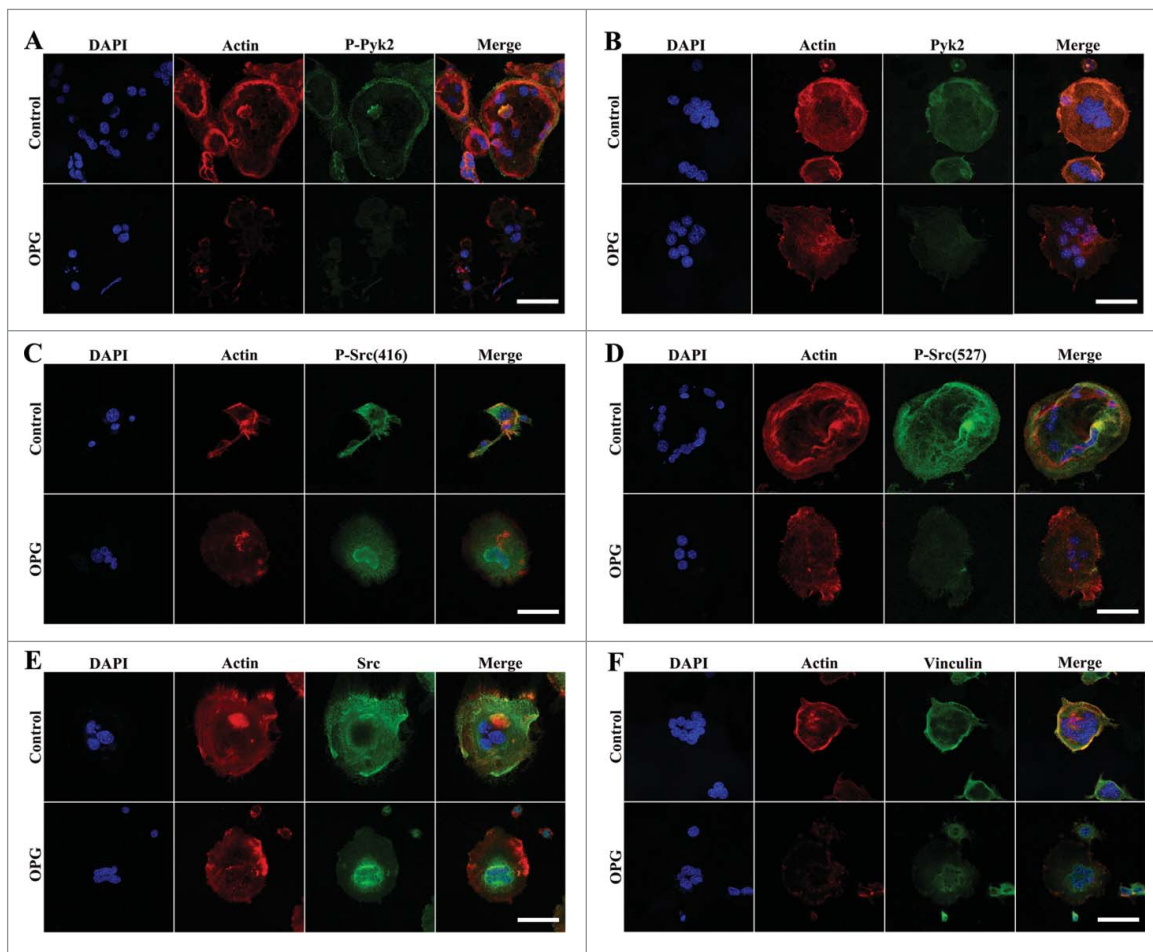


Figure 4. Effects of OPG on osteoclast morphology and distribution of Pyk2, Src and vinculin in OCs. Cells were plated and cultured on coverslips as described in the Methods. Cells treated with 40 ng/mL OPG for 24 h (lower images), or untreated (upper images), were fixed and stained for DAPI, F-actin and either p-Pyk2 402, Pyk2, p-Src(416), p-Src(527), Src or vinculin and examined by confocal immunofluorescence microscopy. (B, E, F) In untreated OCs, Pyk2, Src and vinculin were enriched in the peripheral actin-rich ring. Treatment with OPG for 24 h disrupted the peripheral actin ring and induced the redistribution of all 3 proteins to a more diffuse pattern throughout the cell interior. (A, C, D) OPG-induced signaling modulated Pyk2 and Src tyrosine phosphorylation states, causing a decrease in Tyr 402 Pyk2 and Tyr 527 Src labeling and an increase in Tyr 416 Src labeling at peripheral and central regions. OPG disrupted their co-localization with podosome in both regions. Scale bar = 20 μ m.

the control group (Fig. 5A, B upper panels). OPG treatment increased their colocalization in the central region of OCs where did nuclei distribute (Fig. 5A, B lower panels), which showed increase of Src/Pyk2 association in OCs.

These results were consistent with those in Figure 3 which showed decreased phosphorylated Tyr 402 Pyk2, Tyr 527 Src and increased Src Tyr 416 phosphorylation after OPG treatment in OCs.

Discussion

RAW264.7 cells have been extensively used as *in vitro* OC precursor models.²² In the present study, RAW264.7 cells were cultured in the presence of M-CSF and RANKL.²⁰ TRAP staining was utilized to observe the effects of OPG

on differentiation of OCs using inverted phase contrast microscopy. OPG reduced the number of TRAP-positive OCs in a dose-dependent manner, suggesting that OPG inhibited RAW264.7 cells from differentiating into mature OCs. We used SEM and RTCA to analyze how OPG induces the disruption of the adhesion structure in living OCs. OPG induced retraction of adhesive structures in the peripheral region, detaching OCs from the extracellular substrate and reducing NCI. Results from confocal microscopy and Western blot analysis indicated that the degree of tyrosine phosphorylation in Pyk2 decreased with OPG treatment. OPG induced Src, Pyk2 and vinculin relocation from the peripheral adhesive zone to the central region of OCs. OPG induced a decrease in Pyk2 Tyr 402 and Src Tyr 527 phosphorylation in the peripheral adhesive region.

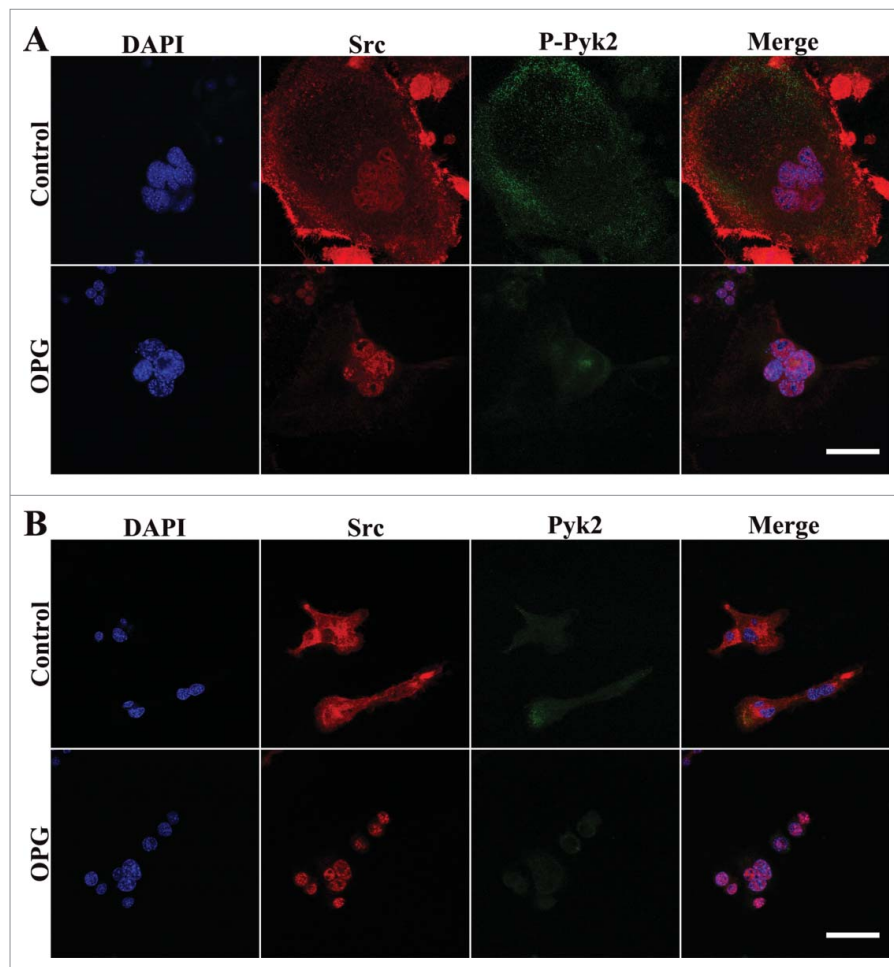


Figure 5. The increase of Src/Pyk2 association in OCs after OPG treatment. Cells were plated and cultured on coverslips as described in the Methods. Cells treated with 40 ng/mL OPG for 24 h (lower images), or untreated (upper images), were fixed and stained for DAPI, Src and either p-Pyk2 402 or Pyk2 and examined by confocal immunofluorescence microscopy. (A) Distribution of p-Pyk2 402 and Src. (B) Distribution of Pyk and Src. OPG treatment enhanced the colocalization of Pyk2 and Src in the central region of OCs. Scale bar = 20 μm .

OPG induced a marked increase in phosphorylation of Tyr 416 Src in the central region of OCs.

TRAP, an OC differentiation marker, as well as cathepsin K, affect the functional activity of OCs by regulating bone matrix resorption and collagen turnover. TRAP-specific staining is widely used to identify OCs *in vivo* and *in vitro* due to its simplicity and ease of manipulation.²³ Previously, we found that RAW264.7 cells cultured in the presence of M-CSF and RANKL for 3 days formed large, mature OCs and OPG inhibited M-CSF and RANKL-induced osteoclastogenesis.²⁰ In the present study, OPG reduced the number of mature OCs characterized as TRAP-positive multinucleated cells indicating that OPG could inhibit the differentiation of OC precursors and prevent them from forming mature osteoclasts. These results were consistent with previous studies.^{24,25} Differentiation and activation of OC precursor cells into mature (active) OCs requires binding of RANKL to RANK.²⁶ The RANK–RANKL interaction is inhibited by

OPG, which binds to RANKL. RANKL is antagonized by OPG, a member of the TNF superfamily, which functions by binding to and sequestering RANKL, impeding the resorption of bone.²⁷ More recently, the crystal structure of the RANKL/OPG interaction was described.²⁸ In that study, the authors showed that OPG (domains 1–4) is able to interact with RANKL at a 1:1 ratio, blocking the accessibility to important binding sites of RANKL to RANK. In addition to its capacity to inhibit osteoclastogenesis, OPG directly disrupted the formation of F-actin ring in isolated OCs inhibiting osteoclastic bone resorption.²⁹

OCs can adhere to several substrates on which they form distinct F-actin structures. *In vitro*, when adhered to plastic or glass, mature OCs exhibit podosomes similar to monocyte-derived cells such as macrophages or dendritic cells.³⁰ In mature OCs, podosomes are arranged at the cell periphery as a characteristic belt.³¹ Co-staining of OCs for actin and avb3 integrin or

vinculin shows a characteristic “donut” of the latter complex of adhesive proteins enclosing a dense actin core. The area surrounding the actin core is also rich in kinases such as c-Src and Pyk2, and the small GTPases Rho, Rac, and cdc42. Also surrounding the dense actin core is a loose network of F-actin cables known as the actin cloud. Although both the actin core and the actin cloud are essential for proper podosome organization and bone resorption, they appear to be independent structures.¹ OCs lacking the kinase c-Src do not have an actin cloud, while those lacking WIP have no actin core. Ultimately, both molecules are essential for podosome formation, since both c-Src- and WIP-deficient OCs have resorptive defects.^{32,33} When they attach to the mineralized bone matrix or to surfaces mimicking bone, such as apatite collagen complexes that can be resorbed, OCs do not form single podosomes or the peripheral podosome belts typical of cells plated on glass. Instead, these resorptive cells organize an inner actin ring which is the functional unit of the OC membrane at the sealing zone. Although the actin ring in the sealing zone is thicker than in the podosome belt, the molecular components (e.g. avb3, vinculin, c-Src, Pyk2, small GTPases) are the same.³⁴ OPG induces retraction of lamellipodia, which are most sensitive to the OPG treatment and peripheral podosome disruption in OCs. This dynamic process can be easily detected by impedance measurements with the xCelligence system. The xCelligence system is a powerful tool for functional analysis of OCs because of its ability to yield information on the proximity of contact between the cell and the substrate. Applying xCelligence system to our study, we combined examination of living cells with biochemical analyses of lysed cells. It is a novel method of OC investigation reflecting conditions in the body.

It is likely that Pyk2 and its associated proteins including Src might play an important role in the signaling pathway of OPG-induced retraction in OCs and rapid disassembly of podosome in OCs. Deletion of Src significantly alters the distribution of podosomes in OCs, eventually leading to the formation of focal adhesion-like structures. This shift from podosome to focal adhesion correlates with a decrease in the formation and motility of lamellipodia and in cell migration, although it is not possible to determine which occurs first.³⁵ The apparatus controlling Src has 3 components referred to by Harrison as the latch, the clamp, and the switch.³⁶ The SH2 domain binds to phosphotyrosine 527 in the C-terminal tail to form the latch. The clamp is an assembly of the SH2 and SH3 domains behind the kinase domain. The switch is the kinase-domain activation loop; the activation loop can switch between active and inactive conformations. An equilibrium exists between the restrained

and active forms of the enzyme. Since Src activity is strictly regulated, the equilibrium favors the inactive bound conformation. The dormant form of the enzyme is destabilized by dephosphorylation of Tyr 527 and by phosphorylation of the activation loop in Tyr 416.¹⁷ In our study, OPG induced a marked decrease in phosphorylation of Tyr 527 in Src and an increase in phosphorylation of Tyr 416 in Src, suggesting that OPG induces retraction of adhesion structure and distribution of podosomes in OCs by disequilibrating the dormant form of Src.

Pyk2 is found in the sealing zone, and its phosphorylation correlates with the formation of the sealing zone and with OC bone resorption. Deletion of Pyk2 in mice leads to mild osteopetrosis due to impairment of OC function. Pyk2-null OCs were unable to transform podosome clusters into a podosome belt at the cell periphery; instead of a sealing zone only small actin rings were formed, resulting in impaired bone resorption.¹² This finding is consistent with our results, showing that inhibition of Pyk2 activity by OPG treatment causes podosome disassembly in the peripheral region and impairment of OC resorption ability. In OCs, Pyk2 associates with c-Src in an SH2-dependent manner. In Src (-/-) OCs, Pyk2 tyrosine phosphorylation and its kinase activity were markedly reduced, and Pyk2 immunoprecipitated from Src (-/-) OCs was shown to be a direct substrate of c-Src *in vitro*. This suggests that the adhesion-dependent phosphorylation of tyrosine in Pyk2 is mediated by c-Src in OCs *in vivo*.³⁷ Dikic et al.¹⁵ showed that Pyk2 tyrosine phosphorylation depends, in part, on Src kinase activity and is stimulated by Src binding to the autophosphorylated site Tyr 402 on Pyk2. Our results indicated that OPG induced a decrease in tyrosine phosphorylation of Pyk2 and dephosphorylation of Pyk2 Tyr 402 at the peripheral adhesive region. After OPG stimulation, more intracellular labeling of Pyk2 and Src was noted in the central region of OCs. Pyk2 showed colocalization with Src but not with actin-containing podosomes. This finding was similar to calcitonin treatment in OCs, which showed that inhibition of Pyk2 activity by calcitonin treatment causes podosome disassembly in the peripheral region and impairment of OC resorption ability.³⁸ The role of Src in OPG induced retraction may, therefore, be to function as an adaptor protein that competes for Pyk2 and relocates it from the peripheral adhesive zone to the central region of OCs.

In conclusion, our study demonstrates that OPG induces dephosphorylation of Tyr 402 in Pyk2 and decreased labeling of Tyr 402 in Pyk2 in the peripheral adhesion region. OPG induces increased intracellular labeling of Tyr 402 Pyk2, Tyr 416 of Src, dephosphorylation at Tyr 527 of Src, and Pyk2/Src association in the

central region of OCs. Taken together, these data suggest that Src may function as an adaptor protein that competes for Pyk2 and relocates it from the peripheral adhesive zone to the central region of OCs. These results provide further insight into how OPG-induced signaling pathways regulate integrin-mediated OC attachment to the extracellular matrix.

Abbreviations

CI	cell index
DAPI	4'-diamidino-2-phenylindole
DMEM	Dulbecco's modified Eagle's medium
FBS	fetal bovine serum
FAK	focal adhesion kinase
M-CSF	macrophage colony-stimulating factor
OPG	osteoprotegerin
OC	osteoclast
RANKL	receptor activator of NF- κ B ligand
RTCA	real-time cell analyzer
RT	room temperature
SEM	scanning electron microscopy
TNF	tumor necrosis factor
TRAP	tartrate-resistant acidic phosphatase
SDS	sodium dodecyl sulfate
α -MEM	minimum essential medium α

Disclosure of potential conflicts of interest

No potential conflicts of interest were disclosed.

Funding

This study was supported by grants from the National Natural Science Foundation of China (nos. 31172373, 31302154 and 31372495), the Specialized Research Fund for the Doctoral Program of Higher Education (no. 20113250110003), the Priority Academic Program Development of Jiangsu Higher Education Institutions (PAPD) and the Graduate Innovation Project of Jiangsu Province (CXZZ12_0917).

References

- [1] Deborah V. Novack RF. Osteoclast motility: Putting the brakes on bone resorption. *Ageing Res Rev* 2011; 10:54-61; PMID:19788940; <http://dx.doi.org/10.1016/j.arr.2009.09.005>
- [2] Boyle WJ, Simonet WS, Lacey DL. Osteoclast differentiation and activation. *Nature* 2003; 423:337-42; PMID:12748652; <http://dx.doi.org/10.1038/nature01658>
- [3] Wiebe SH, Hafezi M, Sandhu HS, Sims SM, Dixon SJ. Osteoclast activation in inflammatory periodontal diseases. *Oral Dis* 1996; 2:167-80; PMID:8957930; <http://dx.doi.org/10.1111/j.1601-0825.1996.tb00218.x>
- [4] Helfrich MH. Osteoclast diseases and dental abnormalities. *Arch Oral Biol* 2005; 50:115-22; PMID:15721137; <http://dx.doi.org/10.1016/j.archoralbio.2004.11.016>
- [5] Shu G, Yamamoto K, Nagashima M. Differences in osteoclast formation between proximal and distal tibial osteoporosis in rats with adjuvant arthritis: inhibitory effects of bisphosphonates on osteoclasts. *Mod Rheumatol* 2006; 16:343-9; PMID:17164994; <http://dx.doi.org/10.3109/s10165-006-0515-1>
- [6] Lee TH, Fevold KL, Muguruma Y, Lottsfeldt JL, Lee MY. Relative roles of osteoclast colony-stimulating factor and macrophage colony-stimulating factor in the course of osteoclast development. *Exp Hematol* 1994; 22:66-73; PMID:8282061
- [7] Lacey DL, Timms E, Tan HL, Kelley MJ, Dunstan CR, Burgess T, Elliott R, Colombero A, Elliott G, Scully S, et al. Osteoprotegerin ligand is a cytokine that regulates osteoclast differentiation and activation. *Cell* 1998; 93:165-76; PMID:9568710; [http://dx.doi.org/10.1016/S0092-8674\(00\)81569-X](http://dx.doi.org/10.1016/S0092-8674(00)81569-X)
- [8] Baud'huin M, Lamoureux F, Duplomb L, Redini F, Heymann D. RANKL, RANK, osteoprotegerin: key partners of osteoimmunology and vascular diseases. *Cell Mol Life Sci* 2007; 64:2334-50; PMID:17530461; <http://dx.doi.org/10.1007/s00018-007-7104-0>
- [9] Theoleyre S, Wittrant Y, Tat SK, Fortun Y, Redini F, Heymann D. The molecular triad OPG/RANKL/RANKL: involvement in the orchestration of pathological bone remodeling. *Cytokine Growth Factor Rev* 2004; 15:457-75; <http://dx.doi.org/10.1016/j.cytogfr.2004.06.004>
- [10] Makihira S, Mine Y, Nikawa H, Shuto T, Kosaka E, Sugiyama M, Hosokawa R. Immobilized-OPG-Fc on a titanium surface inhibits RANKL-dependent osteoclast differentiation in vitro. *J Mater Sci Mater Med* 2010; 21:647-53; PMID:19834789; <http://dx.doi.org/10.1007/s10856-009-3891-1>
- [11] Nakamura I, Duong le T, Rodan SB, Rodan GA. Involvement of $\alpha(v)\beta3$ integrins in osteoclast function. *J Bone Miner Metab* 2007; 25:337-44; PMID:17968485; <http://dx.doi.org/10.1007/s00774-007-0773-9>
- [12] Gil-Henn H, Destaing O, Sims NA, Aoki K, Alles N, Neff L, Sanjay A, Bruzzaniti A, De Camilli P, Baron R, et al. Defective microtubule-dependent podosome organization in osteoclasts leads to increased bone density in Pyk2(-/-) mice. *J Cell Biol* 2007; 178:1053-64.
- [13] Buckbinder L, Crawford DT, Qi H, Ke HZ, Olson LM, Long KR, Bonnette PC, Baumann AP, Hambor JE, Grasser WA 3rd, et al. Proline-rich tyrosine kinase 2 regulates osteoprogenitor cells and bone formation, and offers an anabolic treatment approach for osteoporosis. *Proc Natl Acad Sci U S A* 2007; 104:10619-24; PMID:17537919; <http://dx.doi.org/10.1073/pnas.0701421104>
- [14] Avraham H, Park SY, Schinkmann K, Avraham S. RAFTK/Pyk2-mediated cellular signalling. *Cell Signal* 2000; 12:123-33; PMID:10704819; [http://dx.doi.org/10.1016/S0898-6568\(99\)00076-5](http://dx.doi.org/10.1016/S0898-6568(99)00076-5)
- [15] Dikic I, Tokiwa G, Lev S, Courtneidge SA, Schlessinger J. A role for Pyk2 and Src in linking G-protein-coupled receptors with MAP kinase activation. *Nature* 1996; 383:547-50; PMID:8849729; <http://dx.doi.org/10.1038/383547a0>
- [16] Schlaepfer DD, Hauck CR, Sieg DJ. Signaling through focal adhesion kinase. *Prog Biophys Mol Biol* 1999; 71:435-78; PMID:10354709; [http://dx.doi.org/10.1016/S0079-6107\(98\)00052-2](http://dx.doi.org/10.1016/S0079-6107(98)00052-2)

- [17] Jr. RR. Src protein-tyrosine kinase structure and regulation. *Biochem Biophys Res Commun* 2004; 324:1155-64; PMID:15504335
- [18] Brown MT, Cooper JA. Regulation, substrates and functions of src. *Biochim Biophys Acta* 1996; 1287:121-49; PMID:8672527
- [19] Zheng XM, Resnick RJ, Shalloway D. A phosphotyrosine displacement mechanism for activation of Src by PTPalpha. *EMBO J* 2000; 19:964-78; PMID:10698938; <http://dx.doi.org/10.1093/emboj/19.5.964>
- [20] Fu YX, Gu JH, Zhang YR, Tong XS, Zhao HY, Yuan Y, et al. Inhibitory effects of osteoprotegerin on osteoclast formation and function under serum-free conditions. *J Vet Sci* 2013; 14:405-12; PMID:23820214; <http://dx.doi.org/10.4142/jvs.2013.14.4.405>
- [21] Lakkakorpi PT, Bett AJ, Lipfert L, Rodan GA, Duong le T. PYK2 autophosphorylation, but not kinase activity, is necessary for adhesion-induced association with c-Src, osteoclast spreading, and bone resorption. *J Biol Chem* 2003; 278:11502-12; PMID:12514172; <http://dx.doi.org/10.1074/jbc.M206579200>
- [22] Cuetara BL, Crotti TN, O'Donoghue AJ, McHugh KP. Cloning and characterization of osteoclast precursors from the RAW264.7 cell line. *In Vitro Cell Dev Biol Anim* 2006; 42:182-8; PMID:16948499; <http://dx.doi.org/10.1290/0510075.1>
- [23] Nakayama T, Mizoguchi T, Uehara S, Yamashita T, Kawahara I, Kobayashi Y, Moriyama Y, Kurihara S, Sahara N, Ozawa H, et al. Polarized osteoclasts put marks of tartrate-resistant acid phosphatase on dentin slices—a simple method for identifying polarized osteoclasts. *Bone* 2011; 49:1331-9; PMID:21983021; <http://dx.doi.org/10.1016/j.bone.2011.09.045>
- [24] Xiong Q, Zhang LC, Zhang LH, Yao Q, Tang P. Effects of recombinant human osteoprotegerin and recombinant RANK protein on the differentiation of osteoclast precursors. *Chin J Orthop Traumatol* 2013; 26:324-7.
- [25] Wang X, Luo Y, Liao WB, Zhang J, Chen TM. Effect of osteoprotegerin in combination with interleukin-6 on inhibition of osteoclast differentiation. *Chin J Traumatol* 2013; 16:277-80; PMID:24103822
- [26] Lum L, Wong BR, Josien R, Becherer JD, Erdjument-Bromage H, Schlondorff J, Tempst P, Choi Y, Blobel CP. Evidence for a role of a tumor necrosis factor- α (TNF- α)-converting enzyme-like protease in shedding of TRANCE, a TNF family member involved in osteoclastogenesis and dendritic cell survival. *J Biol Chem* 1999; 274:13613-8; PMID:10224132; <http://dx.doi.org/10.1074/jbc.274.19.13613>
- [27] Bekker PJ, Holloway D, Nakanishi A, Arrighi M, Leese PT, Dunstan CR. The effect of a single dose of osteoprotegerin in postmenopausal women. *J Bone Miner Res* 2001; 16:348-60; PMID:11204435; <http://dx.doi.org/10.1359/jbmr.2001.16.2.348>
- [28] Luan X, Lu Q, Jiang Y, Zhang S, Wang Q, Yuan H, Zhao W, Wang J, Wang X. Crystal structure of human RANKL complexed with its decoy receptor osteoprotegerin. *J Immunol* 2012; 189:245-52; PMID:22664871; <http://dx.doi.org/10.4049/jimmunol.1103387>
- [29] Hakeda Y, Kobayashi Y, Yamaguchi K, Yasuda H, Tsuda E, Higashio K, Miyata T, Kumegawa M. Osteoclastogenesis inhibitory factor (OCIF) directly inhibits bone-resorbing activity of isolated mature osteoclasts. *Biochem Biophys Res Commun* 1998; 251:796-801; PMID:9790989; <http://dx.doi.org/10.1006/bbrc.1998.9523>
- [30] Frederic Saltel AC, Edith Bonnelye, Pierre Jurdic. Actin cytoskeletal organisation in osteoclasts: A model to decipher transmigration and matrix degradation. *Eur J Cell Biol* 2008; 87:459-68; PMID:18294724; <http://dx.doi.org/10.1016/j.ejcb.2008.01.001>
- [31] Destaing O, Saltel F, Geminard JC, Jurdic P, Bard F. Podosomes display actin turnover and dynamic self-organization in osteoclasts expressing actin-green fluorescent protein. *Mol Biol Cell* 2003; 14:407-16; PMID:12589043; <http://dx.doi.org/10.1091/mbc.E02-07-0389>
- [32] Destaing O, Sanjay A, Itzstein C, Horne WC, Toomre D, De Camilli P, Baron R. The tyrosine kinase activity of c-Src regulates actin dynamics and organization of podosomes in osteoclasts. *Mol Biol Cell* 2008; 19:394-404; PMID:17978100; <http://dx.doi.org/10.1091/mbc.E07-03-0227>
- [33] Chabadel A, Banon-Rodriguez I, Cluet D, Rudkin BB, Wehrle-Haller B, Genot E, Jurdic P, Anton IM, Saltel F. CD44 and beta3 integrin organize two functionally distinct actin-based domains in osteoclasts. *Mol Biol Cell* 2007; 18:4899-910; PMID:17898081; <http://dx.doi.org/10.1091/mbc.E07-04-0378>
- [34] Luxenburg C, Geblinger D, Klein E, Anderson K, Hanein D, Geiger B, Addadi L. The architecture of the adhesive apparatus of cultured osteoclasts: from podosome formation to sealing zone assembly. *PLoS One* 2007; 2:e179; PMID:17264882; <http://dx.doi.org/10.1371/journal.pone.0000179>
- [35] Sanjay A, Houghton A, Neff L, DiDomenico E, Bardeley C, Antoine E, Levy J, Gailit J, Bowtell D, Horne WC, et al. Cbl associates with Pyk2 and Src to regulate Src kinase activity, $\alpha(v)\beta(3)$ integrin-mediated signaling, cell adhesion, and osteoclast motility. *J Cell Biol* 2001; 152:181-95; PMID:11149930; <http://dx.doi.org/10.1083/jcb.152.1.181>
- [36] Harrison SC. Variation on an Src-like theme. *Cell* 2003; 112:737-40; PMID:12654240; [http://dx.doi.org/10.1016/S0092-8674\(03\)00196-X](http://dx.doi.org/10.1016/S0092-8674(03)00196-X)
- [37] Duong LT, Lakkakorpi PT, Nakamura I, Machwate M, Nagy RM, Rodan GA. PYK2 in osteoclasts is an adhesion kinase, localized in the sealing zone, activated by ligation of $\alpha(v)\beta(3)$ integrin, and phosphorylated by src kinase. *J Clin Invest* 1998; 102:881-92; PMID:9727056; <http://dx.doi.org/10.1172/JCI3212>
- [38] Shyu JF, Shih C, Tseng CY, Lin CH, Sun DT, Liu HT, Tsung HC, Chen TH, Lu RB. Ru-Band Lu Calcitonin induces podosome disassembly and detachment of osteoclasts by modulating Pyk2 and Src activities. *Bone* 2007; 40:1329-42; PMID:17321230; <http://dx.doi.org/10.1016/j.bone.2007.01.014>